Electronic Supplementary Material (ESI) for Journal of Materials Chemistry A.

Supporting Information

A novel aqueous sodium-manganese battery system for energy storage

Yazhi Feng, [a] *Qiu Zhang,* [a] *Shuang Liu,* [a] *Jian Liu,* [a] *Zhanliang Tao,* *[a,b] *and Jun Chen* [a,b]

[a] Key Laboratory of Advanced Energy Materials Chemistry (Ministry of Education)

College of Chemistry, Nankai University, Tianjin 300071, China.

[b] Renewable Energy Conversion and Storage Center, Nankai University, Tianjin, 300071, P. R. China.

Corresponding Author

* E-mail: taozhl@nankai.edu.cn

Experiment section

Synthesis of $Na_{0.44}MnO_2$ [1]: The $Na_{0.44}MnO_2$ was synthesized by a solid-state reaction method. Mn_2O_3 (98%, Macklin) and Na_2CO_3 (98%, Heowns) were mixed in a molar ratio of 1:0.5 according to a previously reported method. Then the mixture was hand-ground, pelletized, followed by heating at 500℃ for 5 h under air. Then, the pellet was re-ground, re-pelletized, subsequently heated again at 900℃ for 12 h under air. After the two-step calcination the product was obtained.

Hydrophilic treatment of graphite felts (GFs)[2]: graphite felts (GFs) were soaked overnight in acetone (analytical grade, Tianjin reagent co., LTD.), then washed with ultrapure water and ethyl alcohol. After that, 100 mL L^{-1} H_2SO_4 aqueous solution was prepared to solve 200 g L^{-1} ammonium persulfate (96%, Aladdin) followed by adding GFs into above mixture solution and stirred for 15 minutes. Subsequently, GFs were washed by ultrasound in water and ethyl alcohol. Finally, GFs were calcined in Muffle furnace at 450 °C for 30min with heating rate of 5 °C/min.

Electrode fabrication

For $Na_{0.44}MnO_2$ electrode, $Na_{0.44}MnO_2$ powders, super p and poly(vinylidene fluoride) (PVDF) binder were mixed in a mass ratio of 8:1:1 and evenly dispersed in N-methyl-2-pyrrolidone (NMP) to form slurries. Then, the obtained homogeneous slurry was pasted onto a graphite felt and dried at 110 °C for 10 h under a vacuum condition. The mass loading of active material on each current collector was controlled to be about 22 mg cm^{-2}.

AC (YEC-8A) electrode was prepared by mixing the active materials, Ketjen Black, and poly(tetrafluoroethylene) (PTFE, 10 wt % emulsion) onto stainless steel mesh in a weight ratio of 8 :

1 : 1. The mass loading of active material on each current collector was about 29 mg cm^{-2}.

Battery assembly

For single electrode testing, the electrochemical properties were measured in a three-electrode system, with a Pt foil as counter electrode and an Ag/AgCl as reference electrode in 1 M $MnSO_4$ + 1 M Na_2SO_4 + 0.1 M H_2SO_4 aqueous solution. Full-cell batteries were also assembled in three-electrode setup with MnO_2-GF as cathode and AC as anode. Deaerated $MnSO_4$/Na_2SO_4/H_2SO_4 mixed solution obtained through Ar gas bubbling for at least 30 min was used as electrolytes. Only the full cell used for Raman spectrum test and the test of energy density were assembled into a coin cell CR2032 with GF as cathode, filter paper separator, and AC as anode, respectively.

Characterization and electrochemical measurements

X-Ray diffraction (XRD) analysis was performed on a RigakuMiniFlex600 with Cu-Kα radiation (λ = 1.5406 Å) with a rate of 4° min^{-1}. The morphology and structure were observed by field-emission scanning electron microscopy (SEM, JEOL JSM7500F) and transmission electron microscopy (TEM, Philips Tecnai-F20). Raman spectroscopy was measured with a Thermo-Fisher Scientific (excitation wavelength, 532 nm). X-ray photoelectron spectroscopy(XPS) was measured in a Versa Probe PHI 5000 system (Al Kα radiation of 1486.6 eV). The hydrophilicity of graphite felts were convinced by Contact Angle Apparatus (TUB 100). The cyclic voltammetry (CV) is measured using a Parstat 263A electrochemical workstation (AMETEK). Galvanostaic charge/discharge tests are performed on a LAND battery-test instrument (CT2001A). The formula weight for the charged product was tested by electrochemical quartz crystal microbalance (EQCM, QCM 922).

Supplementary Figures

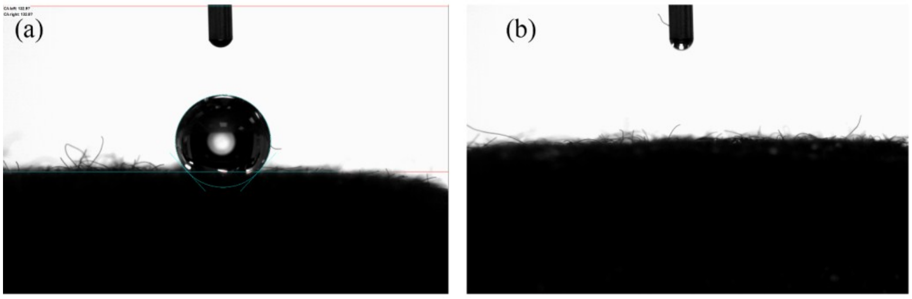

Figure S1. Contact angle images of GF (a) before and (b) after hydrophilic treatment

Table S1. Coulombic efficiency obtained from charge and discharge tests of AC in the 1 M Na_2SO_4, 1 M $MnSO_4$ electrolytes with different concentration of H_2SO_4 in a three-electrode configuration. The charge cut-off voltage is 0.3 V.

Voltage Concentration	0.1 V	0 V	-0.1 V	-0.2 V	-0.3 V	-0.4 V	-0.5 V
0.05 M	98 %	98.75	98.64	98.38	97.79	97.12	96.55
0.1 M	/	99.14	99.30	99.06	98.69	98.47	96.88
0.5 M	/	100.2	99.50	98.15	97.61	95.82	91.00

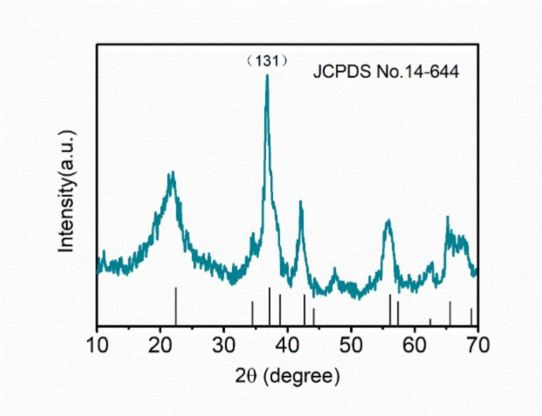

Figure S2. XRD pattern of black powders falling off from the Pt counter electrode in charge-discharge test of AC anode by three-electrode system. It is indexed to gamma-MnO_2 (JCPDS No. 14-644).

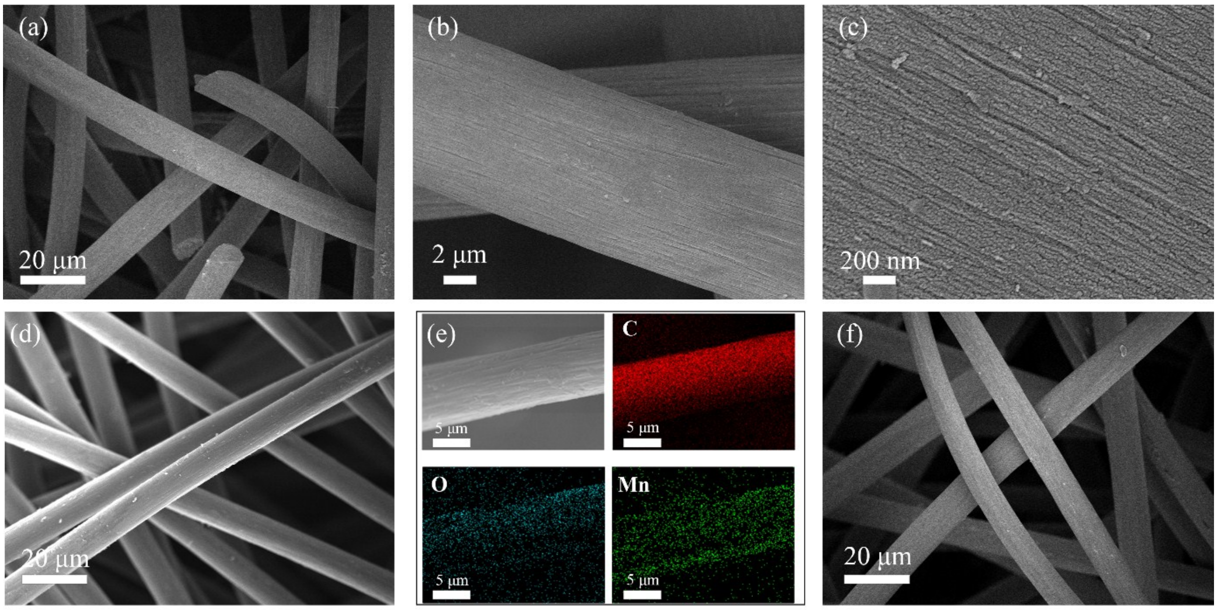

Figure S3. (a, b, c) SEM images of GFs at pristine state. (d) Low-magnification SEM images and (e) EDS elemental mappings of GFs at charged state. (f) Low-magnification SEM images of GFs at discharged state.

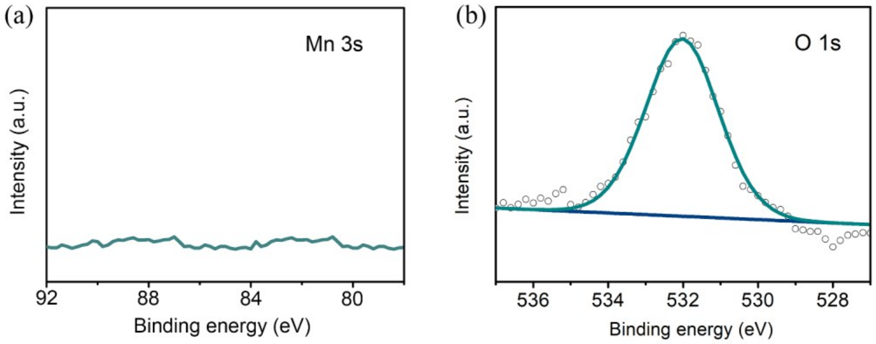

Figure S4. (a) Mn 3s and (b) O 1s XPS records of the cathode at discharged state.

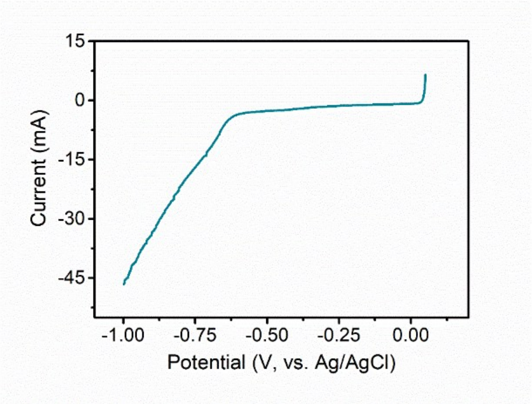

Figure S5. Hydrogen evolution test of AC anode. Cyclic voltammetry curve of AC tested by three-electrode system to detect hydrogen evolution reaction.

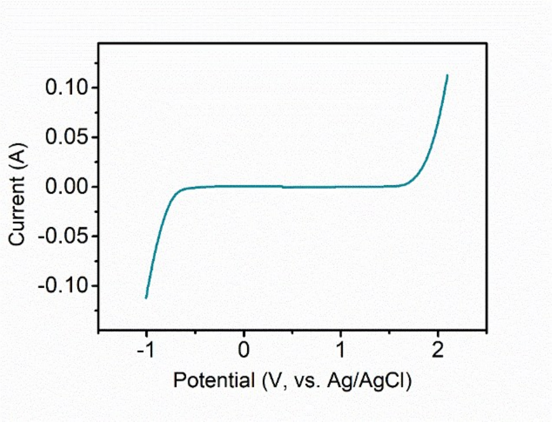

Figure S6. The electrochemical window of the electrolyte of 1 M Na_2SO_4 with 0.1 M H_2SO_4. The measurement was tested at a scan rate of 10 mV s^{-1}.

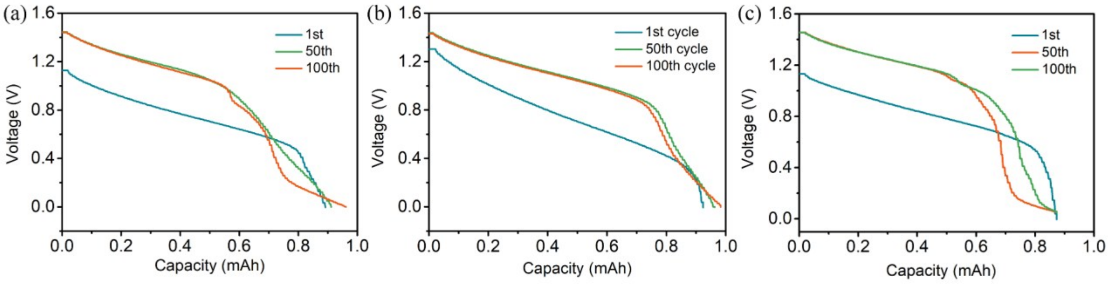

Figure S7. The discharge curves of the full battery in the 1 M Na_2SO_4, 1 M $MnSO_4$ electrolytes with (a) 0.05 M, (b) 0.1 M and (c) 0.5 M H_2SO_4.

Severe capacity decay was observed in 0.5 M H_2SO_4, while 0.05 M is too low to realize reversibility of the reaction of cathode. And there are some corrosion issues in the electrolyte with 0.5 M H_2SO_4, thus the concentration of 0.1 M H_2SO_4 was selected at last.

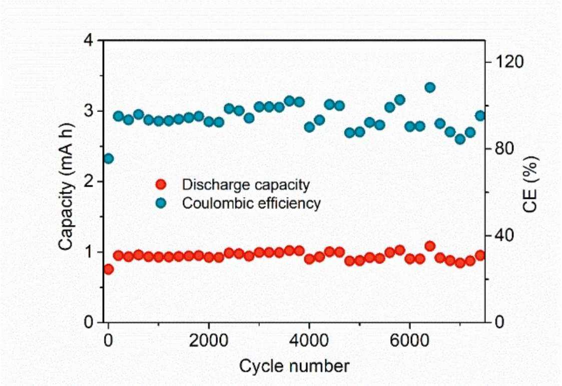

Figure S8. The cycle performance of the full battery in the electrolyte of 1 M Na_2SO_4+$MnSO_4$ with 0.05 M H_2SO_4.

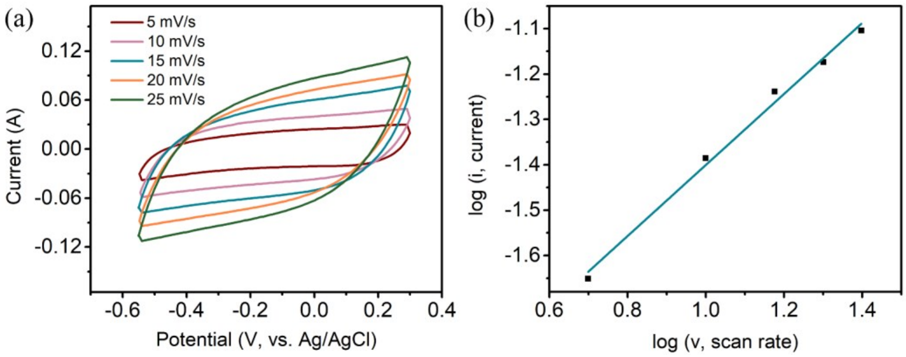

Figure S9. (a) CV curves at different scan rates and (b) corresponding log *i* versus log *v* plots at mid-value potential (current: *i*, scan rate: *v*) of the AC anode.

Figure S9a exhibits CV curves of AC between -0.55 and 0.3 V at different scan rates. According to previous studies, i and v have a relationship like the following equations

$$i = av^b \qquad (1)$$

$$\log(i) = b \times \log(v) + \log(a) \qquad (2)$$

where a and b are adjustable parameters. If b is equal to 1, the electrochemical system is controlled by pseudocapacitance. As b value is 0.5, the ionic diffusion dominates the charge–discharge process. Figure S9b displays log (i) versus log (v) plots at the mid-value potential. The b values is 0.78, suggesting the charge/discharge processes of AC include partial pseudocapacitive behaviors. It leads to a fast Na^+ adsorption/desorption and durable cyclic stability.

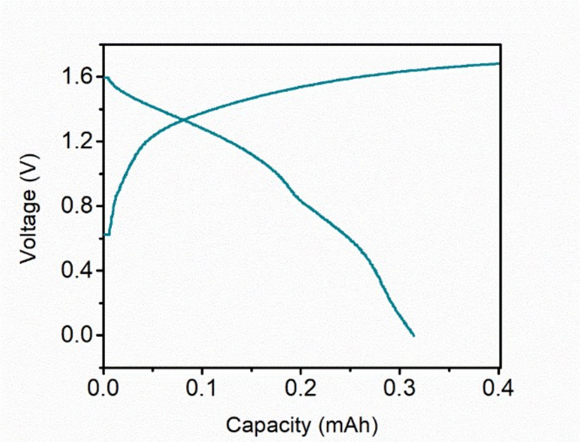

Figure S10. The charge/discharge profile of button cell constructed with graphite felt, filter paper, and active carbon in 1 M Na_2SO_4+$MnSO_4$ with 0.1 M H_2SO_4.

The cell was charged to 0.402 mAh at 2 mA cm^{-2} and discharged to 0 V at 2 mA cm^{-2}.

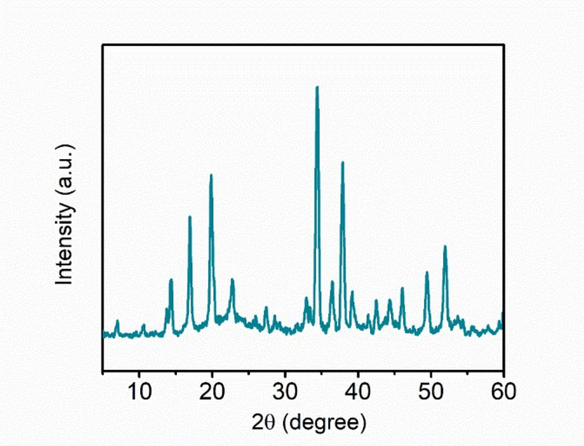

Figure S11. XRD patterns of the synthetic $Na_{0.44}MnO_2$, corresponding to JCPDS No. 27-0750.

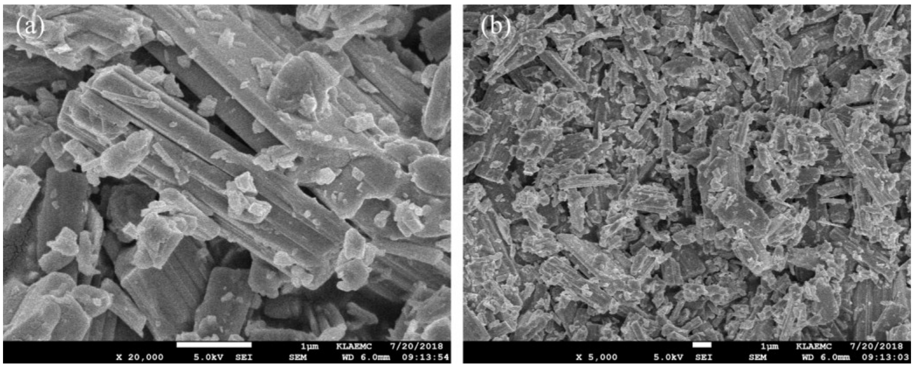

Figure S12. SEM images of $Na_{0.44}MnO_2$. The samples possess irregularity morphology with several micrometers in particle size.

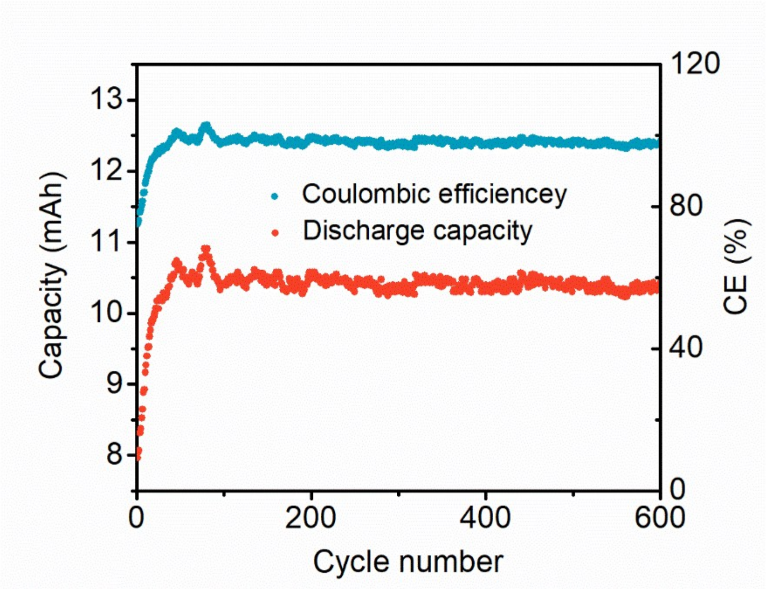

Figure S13. Cycle performance of $MnO_{1.75}$-GF//AC battery with charging at 10 mA cm^{-2} to 10.6 mAh cm^{-2} and discharging at 10 mA cm^{-2} to 0 V.

Table S2. Summary of the electrochemical properties of manganese-based oxides in some typical full cell configurations for ASIBs.

Cathode	Anode	electrolyte	Current rate	Voltage (V)	Capacity mA h g^{-1}	Retention %/cycles	Ref.
$Na_{0.44}MnO_2$	$NaTi_2(PO_4)_3$	1M Na_2SO_4	5 C	1.1	95	86% (100)	3
$Na_{0.66}[Mn_{0.66}Ti_{0.34}]O_2$	$NaTi_2(PO_4)_3$	1M Na_2SO_4	2 C	1.2	76	87% (300)	4
$NaMnO_2$	$NaTi_2(PO_4)_3$	2M CH_3COONa	5 C	1.0	27	75% (500)	5
$K_{0.27}MnO_2$	$NaTi_2(PO_4)_3$	1M Na_2SO_4	0.2 A g^{-1}	1.2	68.5	No decay (100)	6
$Na_3MnTi(PO_4)_3$	$Na_3MnTi(PO_4)_3$	1M Na_2SO_4	1 C	1.4	56.5	98% (100)	7
$Na_{0.44}MnO_2$	Polymide-MNCNT	1M Na_2SO_4	5 C	0.8	60	No decay (200)	8
$Na_{0.44}MnO_2$	$Na_2V_6O_{16}$•nH_2O	1M Na_2SO_4	0.04 A g^{-1}	0.8	30	67% (250)	9
$Na_{0.44}MnO_2$	$NaV_3(PO_4)_3$@C	1M Na_2SO_4	5 C	0.7	100	83% (500)	10
$Na_{0.35}MnO_2$	PPy@MoO_3	0.5M Na_2SO_4	0.55 A g^{-1}	0.8	25	79% (1000)	11
$Na_{0.44}MnO_2$	AC	1M Na_2SO_4	4 C	1.2	25	100% (1000)	12
$MnO_{1.75}$-GF	AC	1M $MnSO_4$, 1M Na_2SO_4 0.1M H_2SO_4	0.2 A cm^{-2}	1.2	147*	~100% (7000)	This work

*based on the mass of 1 cm^2 graphite felt

References

[1] C. H. Wang, Y. W. Yeh, N. Wongittharom, Y. C. Wang, C. J. Tseng, S. W. Lee, W. S. Chang, J. K. Chang, *J. Power Sources*, **2015**, *274*, 1016-1023.

[2] H. Zhou, Y. Shen, J. Xi, X. Qiu, L. Chen, *ACS Appl. Mater. Interfaces*, **2016**, *8*, 15369.

[3] Z. Li, D. Young, K. Xiang, W. C. Carter, Y. M. Chiang, *Adv. Energy Mater.*, **2013**, *3*, 290-294.

[4] Y. Wang, L. Mu, J. Liu, Z. Yang, X. Yu, L. Gu, Y. S. Hu, H. Li, X. Q. Yang, L. Chen, *Adv. Energy Mater.*, **2015**, *5*, 1501005.

[5] Z. Hou, X. Li, J. Liang, Y. Zhu, Y. Qian, *J. Mater. Chem. A*, **2015**, *3*, 1400-1404.

[6] Y. Liu, Y. Qiao, W. Zhang, X. U. Henghui, L. I. Zhen, Y. Shen, L. Yuan, H. U. Xianluo, X. Dai, Y. Huang, *Nano Energy*, **2014**, *5*, 97-104.

[7] H. Gao, J. B. Goodenough, *Angewandte Chemie*, **2016**, *128*, 12960-12964.

[9] C. Deng, S. Zhang, Z. Dong, Y. Shang, *Nano Energy*, **2014**, *4*, 49-55.

[10] L. Ke, J. Dong, B. Lin, T. Yu, H. Wang, S. Zhang, C. Deng, *Nanoscale*, **2017**, *9*, 4183

[11] Y. Liu, B. H. Zhang, S. Y. Xiao, L. L. Liu, Z. B. Wen, Y. P. Wu, *Electrochim. Acta*, **2014**, *116*, 512-517.

[12] J. F. Whitacre, A. Tevar, S. Sharma, *Electrochem. Commun.*, **2010**, *12*, 463-466.